

# In Situ Characterization of Spinel Nanoceramic Suspensions

Tamar Kadosh,<sup>‡,¶</sup> Yachin Cohen,<sup>§</sup> Yeshayahu Talmon,<sup>§</sup> and Wayne D. Kaplan<sup>‡,\*</sup>

<sup>‡</sup>Department of Materials Science & Engineering, Technion – Israel Institute of Technology, Haifa 32000, Israel

<sup>§</sup>Department of Chemical Engineering, Technion – Israel Institute of Technology, Haifa 32000, Israel

<sup>¶</sup>Rafael Ltd., Department M4, Advanced Materials, P.O.B. 2250, Haifa 31021, Israel

**In this study, an approach to characterize ceramic colloidal suspensions has been developed, based on vitrification of aqueous ceramic suspensions and microstructural characterization using cryogenic-temperature scanning electron microscopy (cryo-SEM), augmented by conventional rheological measurements. The flocculation phenomenon in as-milled and aged Mg-spinel (MgAl<sub>2</sub>O<sub>4</sub>) aqueous suspensions was characterized. A microstructure based on hard particle agglomerates separated by long-chain deflocculant molecules was directly observed, and correlated to the rheological properties of the suspension. Several levels of flocculation were detected as a function of suspension preparation conditions. Although suspensions at solid-loading levels appropriate for ceramic processing cannot be characterized using conventional particle size measurement techniques, cryo-SEM can be used to measure characteristic sizes, and to distinguish between agglomerated and flocculated particles, opening a new approach for optimizing solid-loading conditions for slip casting in terms of viscosity and green density.**

## I. Introduction

TRANSPARENT polycrystalline ceramics have received much attention in recent years, due to their applications in systems requiring a combination of optical properties with high material strength and impact resistance. Magnesium aluminate spinel (MgAl<sub>2</sub>O<sub>4</sub>) is one of the most favorable candidates, both for armor and optical applications. Spinel is superior to AlON and sapphire (single crystal  $\alpha$ -Al<sub>2</sub>O<sub>3</sub>) in terms of transmission in the infra-red range (3–5  $\mu$ m).<sup>1</sup> It also has better ballistic efficiency, and a lower predicted cost of production compared with sapphire.<sup>2</sup>

Nonsintered (green) compacts of spinel are commonly produced using the dry-press method,<sup>3,4</sup> but can also be produced using “wet” methods such as slip casting<sup>5,6</sup> or gel casting.<sup>7</sup> The latter methods provide a variety of possible geometries, such as curved windows and domes, which are difficult to form using dry-press methods. An additional advantage of wet methods is the potential to obtain more homogeneously packed green compacts, due to the greater ease with which the particles can slide over one another and rearrange in the wet state.<sup>8</sup> A homogeneous microstructure in the green state is extremely important when transparency in the fully sintered state is required, as heterogeneities (defects) introduced in any stage of the fabrication process can detrimentally affect densification.<sup>9,10</sup> The degree of optical transmission through polycrystalline ceramics strongly

depends on absorption and scattering by pores,<sup>2</sup> making removal of residual porosity a critical step of the sintering process.

The key for successful wet-forming, and the minimization of heterogeneities in the green state, is the ability to produce a well-dispersed, high solid content, low viscosity suspension.<sup>11</sup> These requirements are problematic when submicrometer (nano) ceramic powders are used, due to their high specific surface area, which promotes flocculation. A floc is an agglomerate with a porous microstructure, which forms in a liquid suspension.<sup>12</sup> The particles of a floc are held together by long-range van der Waals forces,<sup>13</sup> or by organic flocculation agents.<sup>9</sup> The surface chemistry of the suspended particles can also affect flocculation. The phenomenon of hydrolysis at the particles’ surface was investigated by Ganesh *et al.* They found that flocculation and coagulation of Mg-spinel aqueous suspensions at solid loadings higher than 30 vol% (~60 wt%), are initially caused by powder hydrolysis.<sup>6,14</sup> Agglomeration and flocculation may lead to porous, poorly packed green structures and reduced green densities.<sup>15</sup>

It is known that flocculation causes an apparent rheological behavior of increasing viscosity with time, often termed “aging.”<sup>16</sup> For this reason, viscosity measurements can indicate the level of flocculation.<sup>14</sup> Despite flocculation phenomenon being well-established for ceramic suspensions in the literature, to the best of the authors’ knowledge, it has rarely been directly observed using microscopy.<sup>17,18</sup> Cryogenic scanning electron microscopy (cryo-SEM) is used in biological research, to directly observe the structure of hydrated samples.<sup>19</sup> In materials science, cryo-SEM was used to observe suspensions of polymers (latex),<sup>20</sup> silica,<sup>21,22</sup> and clays.<sup>17,23</sup> Cryogenic microscopy of water-based samples (suspensions) requires vitrification, where the liquid media of the suspension (commonly water) is rapidly cooled to avoid distortion of the sample morphology by ice crystal formation.

The aim of this study is to develop an experimental approach for the characterization of water-based high solid-load suspensions using cryo-SEM, augmented by conventional rheological characterization techniques. The Mg-spinel system was chosen as a test case. This study demonstrates that cryo-SEM can provide a better understanding of the microstructure of suspensions as a function of composition and solid loading, at solid-loading contents for which conventional particle size measurement tools are not applicable. A secondary goal was to characterize diluted suspensions, and to evaluate the size distribution of primary particles.

## II. Experimental Methods

### (1) Preparation of Suspensions

High purity (99.9%) MgAl<sub>2</sub>O<sub>4</sub> spinel powder (Baikowski, La Balme-de-Sillingy, France) with a nominal powder size distribution (provided by the manufacturer) of  $d_{50} = 0.21 \mu$ m was used as a starting material. De-ionized water (18 M $\Omega$ ) was used for the suspension. Ammonium

A. Krell—contributing editor

Manuscript No. 31106. Received February 22, 2012; approved June 13, 2012.

\*Member, The American Ceramic Society.

<sup>†</sup>Author to whom correspondence should be addressed. e-mail: kaplan@tx.technion.ac.il

polyacrylate (R.T. Vanderbilt, Norwalk, CT) was used as a dispersant (5 wt% of the powder). Ammonia and nitric acid were used to adjust the pH of the suspensions. Alumina milling balls (10 mm diameter; Tosoh, Tokyo, Japan) were used for de-agglomeration using ball-milling for 24 h at a suspension/ball ratio of 1 to 6 (by weight).

Impurities in the powder were identified using induced coupled plasma spectroscopy (ICP), and found to be close to those defined by the powder manufacturer (see Table 1). The specific surface area of the powders was determined using the BET method using nitrogen adsorption (Micromeritics Instrument Corporation, Norcross, GA). The particle size distribution was measured using static laser scattering (SLS, Mastersizer; Malvern Instruments, Westborough, MA).

## (2) Characterization Methods

(A) *Zeta Potential Measurements:* Zeta potential measurements were acquired using a NiComp380 ZLS Zeta Potential Analyzer (Particle Sizing Systems, Santa Barbara, CA). The measured suspensions were diluted to ~150 ppm. The pH was adjusted using 0.1 M nitric acid (HNO<sub>3</sub>) and 0.1 M ammonium hydroxide (NH<sub>4</sub>OH). Concentrated acid and base solutions were also used, to avoid excessive dilution.

(B) *Rheological Measurements:* The rheological properties of a fluid provide information concerning its behavior under shear stress exerted at certain intensities and rates, keeping in mind that colloids are usually non-Newtonian systems. Viscosity measurements were performed using a rotary viscometer (Model LVDV-II; Brookfield, Middleboro, MA), based on ASTM standard E-112.<sup>24</sup> Measurements were taken for time durations of minutes to hours, under constant shear rates, and also under increasing and decreasing shear rates. Some of the measurements were performed after “aging”, where the spindle was allowed to rest for a given time while submerged in the suspension, before rotating it.

(C) *Cryo-SEM:* The fundamental concept of Cryo-SEM as applied to this study was to rapidly cool the suspension, followed by high resolution SEM conducted at cryogenic temperatures, such that the morphology of the spinel particles within the microstructure of the suspension could be investigated. While cooling the aqueous ceramic suspension, ice crystal formation can cause distortion of the sample morphology due to volume changes which occur upon crystallization. To avoid the formation of crystalline ice, the suspension must be rapidly cooled. Rapid cooling can form vitrified (amorphous) water, and the morphology of the suspension will then be preserved. Liquid nitrogen is a common cryogen, but for vitrification of water liquid, ethane is preferred due to the higher cooling rate it induces. Sample preparation for Cryo-SEM took place under controlled environmental conditions of temperature and humidity within a dedicated chamber. Special “plunging tweezers” were inserted into the controlled atmosphere chamber for handling the samples, including rapid cooling. A sample cell was assembled inside the chamber, based on a gold planchette placed inside the cavity of the plunging tweezers, and a ~3  $\mu$ L droplet of the investigated suspension was placed on the planchette, followed by a

second gold planchette to close the sample. A copper grid (200 mesh) was also placed between the two gold planchettes, to facilitate fracture of the droplet after vitrification.

Vitrification is a rapid cooling process, which fixates liquids in the vitreous (glass-like) state. During the vitrification process, the tweezers holding the sample are rapidly plunged into a cup filled with cryogen. The chosen cryogen, ethane, was cooled toward its freezing point (−183°C) by pouring gaseous ethane into a container surrounded by a bath of liquid nitrogen (−196°C), which resulted in the transitional formation of liquid ethane. Then, the sample was quickly plunged into the liquid ethane before the ethane froze. This process was designed to prevent distortion of the suspension’s microstructure by crystalline ice formation, such that subsequent SEM micrographs reflect the true microstructure of the original suspension.<sup>25</sup> After thermal fixation, the sample cell was stored in liquid nitrogen.

The vitrified sample was then inserted into a cryo-SEM specimen holder, and transferred to a BAF-060 system (BAL-TEC, AG, Liechtenstein) for preparation of the sample surface prior to SEM. The BAF-060 system was maintained at a vacuum of 0.001 Pa prior to introduction of the sample, and precooled to approximately −170°C. The specimen was then fractured *in-situ*, and thermally etched. Etching is conducted by raising the temperature to −104°C to sublime water and to expose the morphology of the nonvaporized materials (ceramic particles and organic materials). The sublimation time was optimized to expose the floc microstructures and retain their integrity.<sup>26</sup> As the ceramic suspensions are electrically insulating, the vitrified specimens were coated with a thin film of conductive material (platinum and carbon) in the BAF-060 system, to avoid charging under the SEM electron beam. Issman and Talmon describe the details of this procedure.<sup>27</sup>

After coating, the specimens were transferred using a transfer shuttle (VCT100, Leica Microsysteme GmbH, Vienna, Austria), to a precooled cryo-stage, in a dedicated cryogenic high resolution SEM (Ultra Plus HRSEM; Zeiss, Oberkochen, Germany), equipped with a Schottky field-emission electron source. Micrographs were acquired using both secondary electrons (in-lens and Everhart-Thornley detectors) and backscattered electrons, at a relatively low accelerating voltage of 3–3.5 kV and at working distances of 2.8–5 mm.

## III. Results and Discussion

### (1) Powder Characterization – Dry Powder and Diluted Suspensions

According to BET measurements, the specific surface area ( $S_{\text{BET}}$ ) of the powder is 30 m<sup>2</sup>/gr. As mentioned before, particles with such large surface areas tend to agglomerate and flocculate. Assuming that the particles are uniform spheres, their diameter ( $d$ ) can be estimated to be ~55 nm, using a MgAl<sub>2</sub>O<sub>4</sub> density of  $\rho = 3.58$  gr/cm<sup>3</sup> and  $d_{(\text{nm})} = 6/(\rho \cdot 10^3 \cdot S_{\text{BET}})$ . However, static laser scattering measurements of the raw powder present a wide particle size distribution, with two main peaks around 0.4 and 2.2  $\mu$ m (see Fig. 1).

These contradicting results indicate that the powder is agglomerated. The average diameter calculated from the specific surface area is that of the elementary particle, while the size determined from static laser scattering indicates the mean diameter of the agglomerates. Ball-milling reduces agglomeration, by breaking soft agglomerates. The residual hard agglomerates after complete ball-milling had an average size of 170 nm, distributed between 0.08 and 0.5  $\mu$ m (Fig. 1). The narrow size distribution indicates that this is the optimal milling duration for this specific powder. Milling times of less than 24 h are insufficient and may lead to a nonhomogeneous porous structure of the green compact and therefore, residual porosity in the sintered compact.

**Table 1. Impurities in the Initial Spinel Powder, as Determined From ICP**

Element	Concentration (ppm)
Na	10
Ca	5
Fe	10
Si	20

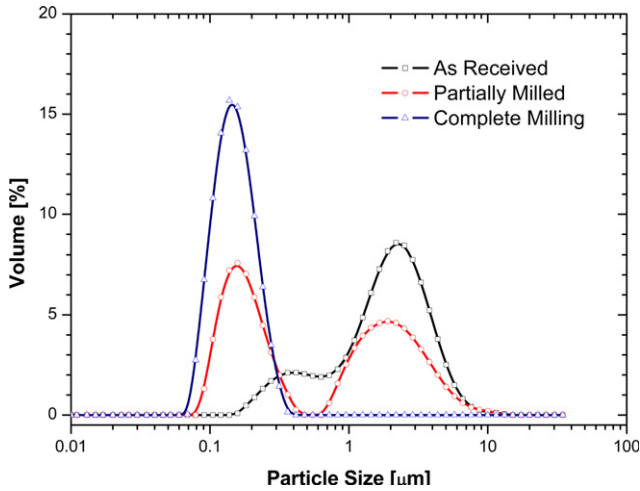
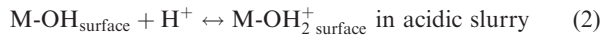


**Fig. 1.** Particle size distribution of the spinel powders, after different times of ball-milling, acquired from static laser scattering (SLS). The particle size determined from the un-milled (raw) powder appears larger than that determined from BET measurements, indicating that the powder is agglomerated. The ball-milling process only partially de-agglomerates the powder, resulting in hard agglomerates with an average diameter of 170 nm.

### (2) Zeta Potential – Diluted Suspensions

Zeta potential measurements can be used to estimate the stability of suspensions in terms of electrical repulsion.<sup>28</sup> When dispersing oxide powders in water, there is a surface reaction leading to the formation of M–OH type hydroxide groups that can dissociate as acids or bases:



The number of negative, neutral, or positive surface sites is of function of pH. At low values of pH, positive surfaces dominate, and vice versa. The net charge density of the particle is determined by sum of the overall surface charge, and can be determined from zeta potential measurements for dilute suspensions.<sup>29</sup>

A dilute (150 ppm) spinel slurry (powder and water) was prepared to find the isoelectric point (IEP) for the powder, where the pH value results in zero net charge density on the surface of the particles.<sup>28</sup> The pH of the slurry was adjusted, while keeping a constant ionic concentration. The IEP was found to be 11.8 (see Fig. 2). This value agrees with values found from other studies.<sup>30,31</sup>

While the determined IEP is not affected by slurry concentration, zeta potential measurements at most values of pH do not necessarily represent the pH required to disperse nondilute slurries (used for casting). For suspensions with high solid-loading, van der Waals forces between particles are more important in defining the stability of the suspension because of the shorter mean distance between particles. The method used in this research employs light for the characterization. Light is scattered from the particles (when they move under an electric field) and to reach the detector, the sample is required to be transparent. Therefore, the original suspension must be diluted and corresponding zeta potential measurements for this (high solid load) suspension were not possible. It should be noted that the zeta potential for high solid-load suspensions have been measured using electroacoustic approaches, but this method is beyond the scope of the current research.<sup>32</sup>

The zeta potential of the investigated (diluted) suspension was measured at different levels of pH to find its IEP. It was found that the isoelectric point shifted to 3.3 upon addition

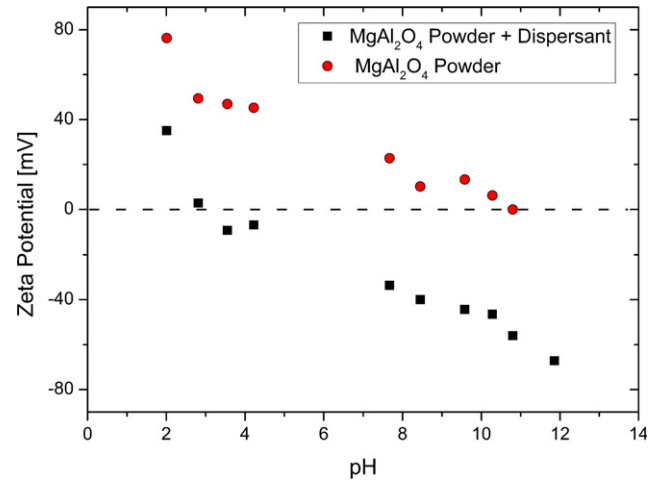


**Fig. 2.** Zeta potential of spinel powder in water and of the investigated spinel suspension (particle concentration of ~150 ppm) at different pH levels. The spinel IEP is at pH~11.8. The IEP of the suspension is pH~3.3. pH values of 10 and higher would provide good dispersion.

of the polyacrylic dispersant (see Fig. 2). Side groups along the polymeric chain dissociate at basic pH values and generate negatively charged sites, whereas the powder, as confirmed using zeta potential measurements, presents a positive net surface charge density at pH values lower than 11.8. The positively charged sites on the powder particles function as anchoring sites for the polymer. The abundant negatively charged groups on the polymer cause the negative values of zeta potential. They repel each other and facilitate the dispersion. According to DLVO theory, a zeta potential greater than  $\pm 40$  mV is necessary to prepare stable aqueous suspensions at high solid loading.<sup>9</sup> A sufficient repulsive force between particles is required to overcome the attractive van der Waals interactions that tend to hold the particles together (forming aggregation and flocculation).<sup>6</sup> Vallar *et al.* stated that absolute values of zeta potential higher than 50 mV can predict good stability of a suspension.<sup>29</sup> Following that, for this study, basic values of pH higher than pH = 10 should provide good dispersion.

### (3) Rheological Measurements – High Solid Load Suspensions

Flocculation is defined as nucleation and growth of particle clusters.<sup>28</sup> As flocculation increases the viscosity of a suspension, a nonflocculated suspension will have a lower viscosity than a flocculated one. The viscosity was measured for a 60 wt% suspension (immediately after milling), while increasing and decreasing the shear rate (see Fig. 3). An inverse relation was found between viscosity and shear rate, where the viscosity decreased as the shear rate was increased. This phenomenon is referred to as shear-thinning or pseudo-plastic behavior, which is well-known in colloidal systems.<sup>9</sup> Low shear rates allow flocculation, whereas higher shear rates break flocs and reduce the viscosity. In other words, the decrease in viscosity with increasing shear rate can be explained by the increased rupture of links between flocs with increasing shear rate, providing easier flow of the liquid.<sup>29</sup> At later stages of the experiment, the viscosity increased. The increased viscosity can be explained by flocculation, which takes place even during the experiment, although the suspension is stirred.

The viscosity of the “fresh” (as-milled) suspension was measured as a function of time under a constant rate of shear (Brookfield spindle number 3 at 60 rpm). “Aging” of the suspension was investigated by vigorously shaking a fresh suspension for at least 10 min, followed by resting the

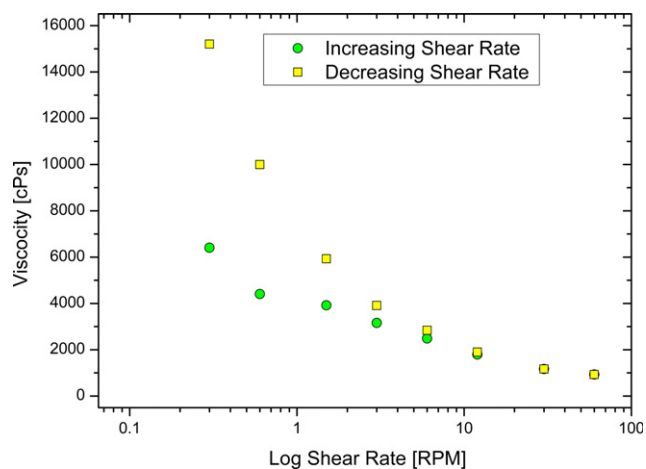


**Fig. 3.** The viscosity versus shear rate for an as-milled 60 wt% spinel suspension at 26°C (using the Brookfield spindle number 3). The suspension is shear thinning (i.e., pseudo-plastic), where the higher the shear rate, the lower the viscosity. During the measurements, the suspension becomes more viscous due to flocculation.

suspension for 20 min (the aging period). Afterward, its viscosity was measured again, as a function of time under a constant rate of shear. Both fresh and aged suspensions showed decreasing and then increasing viscosity with time under a constant shear rate (see Fig. 4). From these results, it may be concluded that aging promotes flocculation of the suspended particles as the attractive forces between particles increases with time. To separate the particles, a higher shear stress is then required. Hence, the viscosity of the aged suspension is initially higher than that of the “fresh” (as-milled) suspension.

For both suspensions (as-milled and aged), the viscosity initially decreases with time under constant shear, as expected from a thixotropic system. Later on, the trend reverses, and the viscosity rises. Although the viscosity eventually rises, the aged suspension can be referred to as thixotropic (an apparent viscosity that decreases with time under shear<sup>9</sup>). The decreasing and then increasing viscosity can indicate that flocs are first broken, and then reformed.

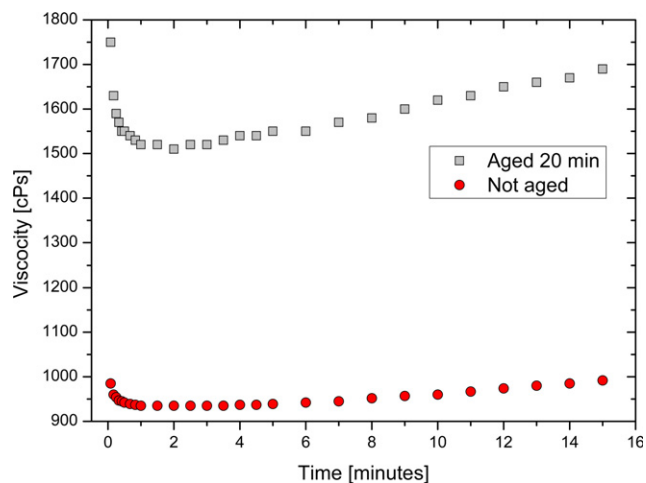


**Fig. 4.** Viscosity versus time for a 60 wt% spinel suspension at 26°C (Brookfield spindle number 3 at 60 rpm). The viscosity decreases and then increases during the measurement, indicating that flocs are first broken and then reformed. The suspension was measured twice: immediately after ball-milling and after 20 min of aging. The aged suspension is significantly more viscous than the suspension immediately after ball-milling.

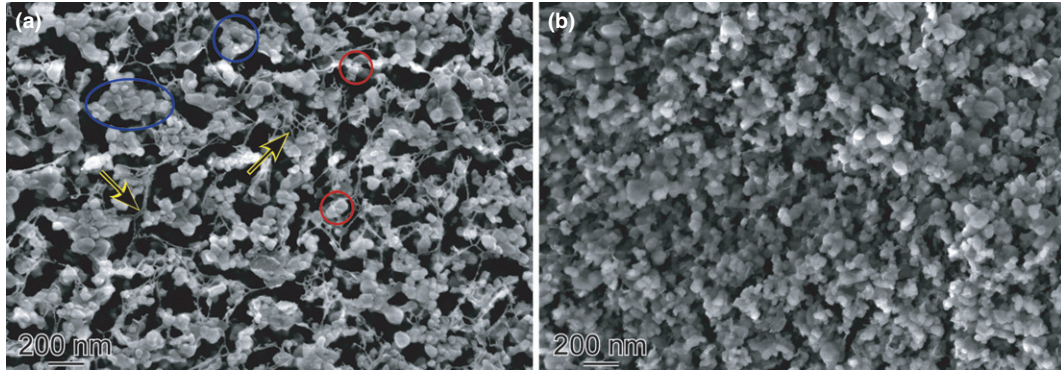
When the suspension is at rest (during aging), the particles move in Brownian motion and collide. When the suspension is stirred during the measurement, the spindle facilitates laminar flow. Particles in a uniform, laminar shear flow collide because of their relative motion. A particle closer to the rotating spindle moving at a higher velocity, overtakes and collides with a slower moving particle, farther from the spindle. Friedlander *et al.* assumed that the Brownian motion (when the suspension is at rest, during the aging period) and laminar shear (when the suspension is stirred) both contribute to flocculation and coagulation, but at higher shear rates, the contribution of the Brownian motion to coagulation can be neglected.<sup>33</sup> Although high shear rates are expected to break-up large flocs, it is expected that the shear stress will increase the collision frequency and hence quickly create large floc aggregates. In addition, higher shear rates may form denser flocs.<sup>34</sup> From these results, it may be concluded that aging promotes flocculation of the suspended particles, as the attractive forces between particles increase with time. To separate the flocs, a higher shear stress is required. Hence, the viscosity of the aged suspension is initially higher than that of the as-milled suspension. A viscosity rise indicates that either the flocs are denser (harder to break-up) or that there are more flocs (the flocculation rate increases). Therefore, the flocs formed by laminar shear are either stronger or more quickly formed than the flocs formed due to Brownian motion at rest. It should be noted that vigorous stirring applied to the aged suspension reduced its viscosity to the initial (nonaged) value.

#### (4) Cryo-SEM – Both Diluted and High Solid Load Suspensions

Specimens of the investigated suspensions were prepared according to the procedure described above. A suspension of 60 wt% solid-loading was ball-milled, after adjusting the pH to greater than 10 (to obtain a good dispersion). The ball-milled suspension was shaken vigorously immediately before preparing the sample [Fig. 5(a)]. The suspension was then aged for half an hour, and another sample was prepared [Fig. 5(b)]. Figure 5 demonstrates that the as-milled suspension is weakly flocculated, whereas the aged sample is heavily flocculated.

Figure 5(a) shows the presence of both agglomerated and flocculated particles. The hard agglomerates (circled) which remain after ball-milling assemble into porous flocs (dashed circles). The regions with dark contrast between the particles are the holes left after water sublimation. The filaments indicated by arrows are bundles of the polymeric dispersant, formed during sublimation before observation, and may imply either a redundant or deficient amount of dispersant in the suspension. An excessive amount of polymer causes “bridging”, or links between the particles, which holds them together, and promotes flocculation.<sup>35</sup> On the other hand, when the amount of dispersant is too low, particle coverage by adsorption of the polymer is incomplete and may also provide a driving force for particles to cluster together.<sup>28</sup> As mentioned earlier, flocculation can also be attributed to hydrolysis at the surface of the particles when they are in contact with water, due to the alkaline nature of Mg-spinel (similar to magnesia), as Ganesh *et al.* suggested.<sup>6,14</sup> Aging is shown herein to promote flocculation. Qualitative differences in the microstructure between the weakly flocculated suspension and the strongly flocculated (aged) suspension can be observed. The weakly flocculated suspension shows a homogeneous structure of separated flocs, whereas the microstructure of the strongly flocculated suspension is rather inhomogeneous with voids between areas of densely packed particles. The seemingly denser structure of the aged suspension is attributed to the multiple levels of particles.

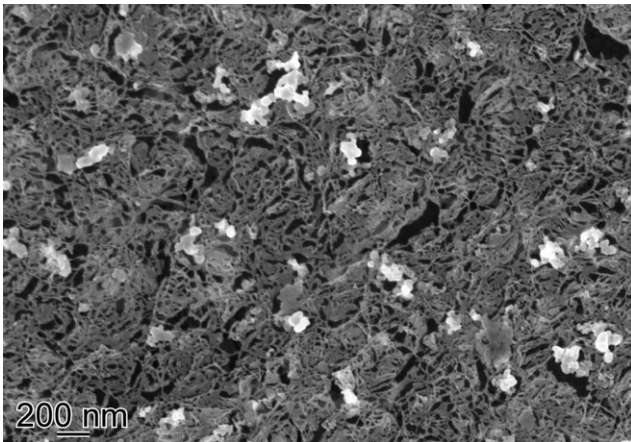
The 60 wt% suspension was diluted to 0.6 wt% and another specimen was prepared for cryo-SEM. As shown in



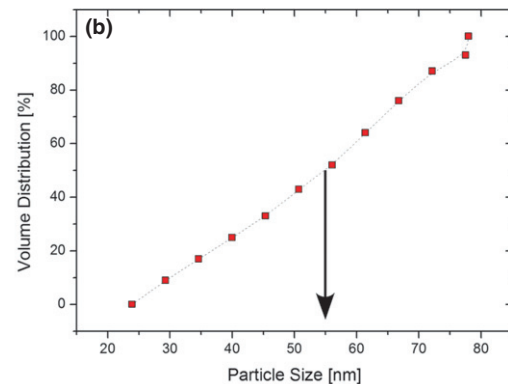
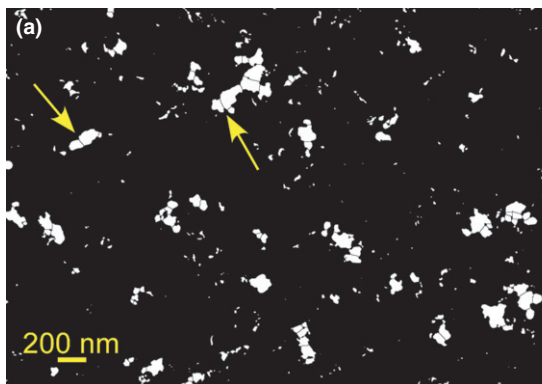
**Fig. 5.** Secondary electron cryo-HRSEM micrographs, based on a combined signal from in-lens and conventional secondary electron detectors, of a 60 wt% spinel suspension (a) without aging; (b) after 0.5 h aging. The suspension in (a) is weakly flocculated, while the aged suspension (b) presents a higher level of flocculation. Flocs are indicated by dashed circles (on-line: blue circles), and residual agglomerates by continuous circles (on-line: red circles). The filaments indicated by arrows are bundles of the polymeric dispersant, formed during sublimation before observation.

Fig. 6, the diluted suspension is well-dispersed. The elementary particles of the powder form hard agglomerates. Those agglomerates are well-dispersed, as expected from suspensions at low solid-loading. The size of the agglomerates was estimated to be between 150 and 200 nm. This result agrees with the results obtained by SLS of the peak around 170 nm. The polymer, presumably with some water adsorbed to it, forms the matrix visible in the background, perhaps as a result of local freezing.

Using image analysis software (ImageJ), the particles detected from micrographs of the diluted suspension (Fig. 6)



**Fig. 6.** HRSEM of a 0.6 wt% suspension diluted from the original 60 wt% suspension. The suspension is nonfloculated and the hard agglomerates are well-dispersed.



**Fig. 7.** (a) The micrograph in Fig. 6 after processing using the ImageJ software. The thin lines, indicated by arrows, are the boundaries between elementary particles in the suspension. (b) Results from image analysis after processing. The median diameter is 55 nm.

were differentiated from the background, and their cross-sectional area was measured (Fig. 7). The diameter of the elementary particles was determined from the cross-sectional area, assuming a spherical shape. The particles' volume was calculated based on the determined diameters. The volume distribution is presented in Fig. 7(b). The particles are distributed between 25 and 80 nm in diameter, while the median diameter is 55 nm. The particle diameter distribution obtained using cryo-SEM imaging of the dilute suspension confirms a median value close to 55 nm, as also expected from BET.

#### IV. Summary and Conclusions

The previously assumed microstructure of a flocculated suspension was confirmed using cryo-SEM of vitrified suspensions, and correlated with flocculation using rheology measurements. Flocculation is affected by several parameters of the suspension. Some of the most critical parameters include additives, such as dispersing agents, solid-loading of the suspension, particle size distribution of the powder, and aging. Flocculation can also be caused by either an excess or deficient amount of dispersant, or a high molecular weight of the dispersant. In this study, an excess amount of polymeric dispersant is probably the source of particle bridging and flocculation.

The initial spinel powder used in this study was heavily agglomerated. Ball-milling was only successful in breaking up the soft agglomerates. The residual hard agglomerates had an average diameter of 170 nm, and were composed of several elementary particles. The structures in the original suspension are flocs, hundreds of nanometers in diameter, and not 170 nm as indicated from light scattering. The

source of this discrepancy is the requirement for dilute suspensions for SLS, making its use limited for characterizing suspensions at solid concentrations relevant for slip casting.

The powder was characterized to have an isoelectric point at pH = 11.8. Acidity (pH) adjustments alone did not disperse the powder in water, although the electric repulsion was high enough according to zeta potential measurements. Polyacrylic dispersants of the group tested, shifted the isoelectric point to pH = 3.3. Zeta potential measurements, which also must be conducted on relatively dilute suspensions, only provides information on electrostatic forces. As a result, the suspension was flocculated, even though the zeta potential measured for the suspension at a pH above 10 predicts good stability.

The investigated spinel suspension was rheologically characterized to be pseudo-plastic, and the aged suspension is also thixotropic. An aging phenomenon of increasing flocculation with time was observed for the submicrometer length-scale powders, requiring an increased shear stress to separate the particles.

The common techniques described in this study, augmented using cryo-SEM, can be applied to characterize other ceramic suspensions and optimize the suspension for specific processing. The advantage of cryo-SEM (combined with viscosity measurements) is that it can be conducted on suspensions having a solid concentration applicable to slip casting, providing direct imaging of the microstructure of the original suspension used for casting.

### Acknowledgments

This research was financially supported by Rafael Ltd. The microscopy was performed at the Electron Microscopy Center for Soft Materials, supported by the Technion Russell Berrie Nanotechnology Institute (RBNI). L. Issman, N. Elisar, L. Ronen and I. Ben-Barak are gratefully acknowledged for assistance during cryo-SEM specimen preparation. D. Gorni, S. Bar-Ziv and A. Shenhar are kindly acknowledged for fruitful discussions and valuable suggestions. The authors are grateful to L. Zisman for performing SLS measurements. G. Shter is acknowledged for performing MIP measurements. S. Brandon and M. Shapira are acknowledged for discussions on particle movement under laminar shear flow.

### References

- <sup>1</sup>J. A. Savage, "Preparation and Properties of Hard Crystalline Materials for Optical Applications - A Review," *J. Cryst. Growth*, **113** [3-4] 698-715 (1991).
- <sup>2</sup>A. Krell, J. Klimke, and T. Hutzler, "Advanced Spinel and Sub- $\mu\text{m}$   $\text{Al}_2\text{O}_3$  for Transparent Armour Applications," *J. Eur. Ceram. Soc.*, **29** [2] 275-81 (2009).
- <sup>3</sup>A. Krell, T. Hutzler, J. Klimke, and A. Potthoff, "Fine-Grained Transparent Spinel Windows by the Processing of Different Nanopowders," *J. Am. Ceram. Soc.*, **93** [9] 2656-66 (2010).
- <sup>4</sup>K. Maca, M. Trunc, and R. Chmelik, "Processing and Properties of Fine-Grained Transparent  $\text{MgAl}_2\text{O}_4$  Ceramics," *Ceram.-Silik.*, **51** [2] 94-7 (2007).
- <sup>5</sup>N. Benameur, G. Bernard-Granger, A. Addad, S. Raffy, and C. Guizard, "Sintering Analysis of a Fine-Grained Alumina-Magnesia Spinel Powder," *J. Am. Ceram. Soc.*, **94** [5] 1388-96 (2011).
- <sup>6</sup>I. Ganesh, "Aqueous Slip Casting of  $\text{MgAl}_2\text{O}_4$  Spinel Powder," *Bull. Mater. Sci.*, **34** [2] 327-35 (2011).
- <sup>7</sup>I. Ganesh, S. M. Olhero, P. M. C. Torres, and J. M. F. Ferreira, "Gelcasting of Magnesium Aluminate Spinel Powder," *J. Am. Ceram. Soc.*, **92** [2] 350-7 (2009).
- <sup>8</sup>J. Binner and B. Vaidyanathan, "Processing of Bulk Nanostructured Ceramics," *J. Eur. Ceram. Soc.*, **28** [7] 1329-39 (2008).
- <sup>9</sup>J. A. Lewis, "Colloidal Processing of Ceramics," *J. Am. Ceram. Soc.*, **83** [10] 2341-59 (2000).
- <sup>10</sup>A. Krell and J. Klimke, "Effects of the Homogeneity of Particle Coordination on Solid-State Sintering of Transparent Alumina," *J. Am. Ceram. Soc.*, **89** [6] 1985-92 (2006).
- <sup>11</sup>Y. Hotta, T. Tsugoshi, T. Nagaoka, M. Yasuoka, K. Nakamura, and K. Watari, "Effect of Oligosaccharide Alcohol Addition to Alumina Slurry and

- Translucent Alumina Produced by Slip Casting," *J. Am. Ceram. Soc.*, **86** [5] 755-60 (2003).
- <sup>12</sup>D. J. Shanefield, in *Organic Additives and Ceramic Processing*, pp. 297-8. 2nd edition, Kluwer Academic Publishers, MA, 1999.
- <sup>13</sup>R. H. French, "Origins and Applications of London Dispersion Forces and Hamaker Constants in Ceramics," *J. Am. Ceram. Soc.*, **83** [9] 2117-46 (2000).
- <sup>14</sup>S. M. Olhero, I. Ganesh, P. M. C. Torres, and J. M. F. Ferreira, "Surface Passivation of  $\text{MgAl}_2\text{O}_3$  Spinel Powder by Chemisorbing  $\text{H}_3\text{PO}_4$  for an Easy Aqueous Processing," *Langmuir*, **24** [17] 9525-30 (2008).
- <sup>15</sup>G. Y. Onoda Jr., L. L. Hench, R. E. Misyler, D. J. Shanefield, and R. B. Runk, "Physical Characterization Terminology"; pp. 36-7 and "Tape Casting of Ceramics"; pp. 418-419 in *Ceramic Processing Before Firing*, Edited by G. Y. Onoda Jr. and L. L. Hench. Wiley-Interscience, Gainesville, 1978.
- <sup>16</sup>O. Lyckfeldt, L. Palmqvist, and E. Carlstrom, "Stabilization of Alumina with Polyelectrolyte and Comb Copolymer in Solvent Mixtures of Water and Alcohols," *J. Eur. Ceram. Soc.*, **29** [6] 1069-76 (2009).
- <sup>17</sup>M. S. Zbik, R. St. C. Smart, and G. E. Morris, "Kaolinite Flocculation Structure," *J. Colloid Interface Sci.*, **328** [1] 73-80 (2008).
- <sup>18</sup>A. Lasalle, C. Guizard, S. Deville, F. Rossignol, and P. Carles, "Investigating the Dispersion State of Alumina Suspensions: Contribution of Cryo-Field-Emission Gun Scanning Electron Microscopy Characterizations," *J. Am. Ceram. Soc.*, **94** [1] 244-9 (2011).
- <sup>19</sup>M. A. Whitelaw-Weckert, E. S. Whitelaw, S. Y. Rogiers, L. Quirk, A. C. Clark, and C. X. Huang, "Bacterial Inflorescence Rot of Grapevine Caused by *Pseudomonas Syringae* pv. *Syringae*," *Plant. Pathol.*, **60** [2] 325-37 (2011).
- <sup>20</sup>H. Luo, L. E. Scriven, and L. F. Francis, "Cryo-SEM Studies of Latex/Ceramic Nanoparticle Coating Microstructure Development," *J. Colloid Interface Sci.*, **316** [2] 500-9 (2007).
- <sup>21</sup>L. Omer, S. Ruthstein, D. Goldfarb, and Y. Talmon, "High-Resolution Cryogenic-Electron Microscopy Reveals Details of a Hexagonal-to-Bicontinuous Cubic Phase Transition in Mesoporous Silica Synthesis," *J. Am. Chem. Soc.*, **131** [34] 12466-73 (2009).
- <sup>22</sup>H. M. Wyss, M. Hutter, M. Muller, L. P. Meier, and L. J. Gauckler, "Quantification of Microstructures in Stable and Gelated Suspensions From Cryo-SEM," *J. Colloid Interface Sci.*, **248** [2] 340-6 (2002).
- <sup>23</sup>M. Zbik, "SEM Evidence of Structural Re-Arrangement From Gelling to Aggregation in Birdwood Kaolinite," *Colloids Surf. A: Physicochem. Eng. Asp.*, **287**, 191-6 (2006).
- <sup>24</sup>ASTM D2196 - 10, *Standard Test Methods for Rheological Properties of Non-Newtonian Materials by Rotational (Brookfield type) Viscometer*. doi: 10.1520/D2196-10, <http://www.astm.org/Standards/D2196.htm>. (accessed 5 July 2012).
- <sup>25</sup>Y. Qi, E. Kesselman, D. J. Hart, Y. Talmon, A. Mateo, and J. L. Zakin, "Comparison of Oleyl and Elaidyl Isomer Surfactant-Counterion Systems in Drag Reduction, Rheological Properties and Nanostructure," *J. Colloid Interface Sci.*, **354** [2] 691-9 (2011).
- <sup>26</sup>J. Du, R. A. Pushkarova, and R. St. C. Smart, "A Cryo-SEM Study of Aggregate and Flocc Structure Changes During Clay Settling and Raking Processes," *Int. J. Miner. Process.*, **93** [1] 66-72 (2009).
- <sup>27</sup>L. Issman and Y. Talmon, "Cryo-SEM Specimen Preparation Under Controlled Temperature and Concentration Conditions," *J. Microsc.*, **246** [1] 60-9 (2012).
- <sup>28</sup>J. Cesarano and I. A. Aksay, "Processing of Highly Concentrated Aqueous  $\alpha$ -Alumina Suspensions Stabilized with Polyelectrolytes," *J. Am. Ceram. Soc.*, **71** [12] 1062-7 (1988).
- <sup>29</sup>S. Vallar, D. Houivet, J. El Fallah, D. Kervadec, and J.-M. Haussonne, "Oxide Slurries Stability and Powders Dispersion: Optimization with Zeta Potential and Rheological Measurements," *J. Eur. Ceram. Soc.*, **19** [6-7] 1017-21 (1999).
- <sup>30</sup>A. Saberi, F. Golestani-Fard, M. Willert-Porada, R. Simon, T. Gerdes, and H. Sarpoalaky, "Improving the Quality of Nanocrystalline  $\text{MgAl}_2\text{O}_4$  Spinel Coating on Graphite by a Prior Oxidation Treatment on the Graphite Surface," *J. Eur. Ceram. Soc.*, **28** [10] 2011-7 (2008).
- <sup>31</sup>H. Zhang, X. Jia, Z. Liu, and Z. Li, "The Low Temperature Preparation of Nanocrystalline  $\text{MgAl}_2\text{O}_4$  Spinel by Citrate Sol-Gel Process," *Mater. Lett.*, **58** [10] 1625-8 (2004).
- <sup>32</sup>A. S. Dukhin and P. J. Goetz, "New Developments in Acoustic and Electroacoustic Spectroscopy for Characterizing Concentrated Dispersions," *Colloids Surf. A: Physicochem. Eng. Asp.*, **192**, 267-306 (2001).
- <sup>33</sup>S. K. Friedlander, "Collision and Coagulation"; pp. 200-2 in *Smoke, Dust, and Haze - Fundamentals of Aerosol Dynamics*, 2nd ed., Edited by S. K. Friedlander. Oxford University Press, NY, 2000.
- <sup>34</sup>I. C. Tse, K. Swetland, M. L. Weber-Shirk, and L. W. Lion, "Fluid Shear Influences on the Performance of Hydraulic Flocculation Systems," *Water Res.*, **45** [17] 5412-8 (2011).
- <sup>35</sup>K. Sato, H. Yilmaz, Y. Hotta, A. Ijuin, and K. Watari, "Dispersion of Ceramic Particles in Aqueous Media with Surface-Grafted Dispersant," *J. Am. Ceram. Soc.*, **92** [1] 256-9 (2009). □